Available online at www.eccomasproceedia.org
Eccomas Proceedia SMART (2023) 1755-1767

ECCOMAS
Proceedia

X ECCOMAS Thematic Conference on Smart Structures and Materials
SMART 2023
D.A. Saravanos, A. Benjeddou, N. Chrysochoidis and T. Theodosiou (Eds)

LARGE STROKE PRE-TWISTED SHEATH-RUN CARBON NANOTUBE ARTIFICIAL MUSCLE FIBER AND THE ACTUATION MECHANISM UNDER WEAK CURRENT

Zeng-hui Zhao, Su-feng Zhu, Xu-feng Dong*, Min Qi

*Key Laboratory of Energy Materials and Devices (Liaoning Province), School of Materials Science and Engineering, Dalian University of Technology, Dalian 116024, China

E-mail: dongxf@dlut.edu.cn

Abstract. Although twisted carbon nanotube (CNT) fibers have the advantages of high actuation speed and high load capacity and have shown potential application value in the field of artificial muscle, their application was still limited by small stroke. In this work, based on the efficient sheath-run structure, the pre-twisted CNT fiber@ Polydimethylsiloxane (PDMS) artificial muscle can produce a tensile stroke of 13.28% at 50 mA which is close to coiled artificial muscles and show fast-running characteristics in circuit control. However, this phenomenon cannot be explained by reported mechanisms under weak electric current because the Joule Heat effect was not noticeable. Herein, we report a novel densification mechanism, which considers that the radial shrinkage stress of the guest sheath during solidification reduces the distance between the inner CNTs. Hence, the collective Ampere force and spiral deformation of CNTs increased. In the range of 25 °C - 40 °C, radiation heating and joule heating were used for stimulation respectively, but the actuation was only generated when the current passes through the core CNT fiber, which indicates that the sheath-run CNT artificial muscle fiber has different working mechanisms in the low-temperature range. The extreme value of the elastic modulus of the core CNT fiber after wrapping the PDMS sheath increased from 118 MPa to 780 MPa and the resistivity was 16% lower, which confirmed that the curing shrinkage stress of the PDMS sheath densify the core CNT fiber and the interaction of inner CNTs increased. In this process, the Ampere force exceeds the elastic deformation energy absorbed by the PDMS sheath, so even if the PDMS sheath does not expand and soften, the actuation performance can be improved by densification. In this article, not only the twisted CNTartificial muscle fiber with large stroke was prepared, but also the working mechanism of sheath-run artificial muscle was supplemented, which provides a new idea for the development of artificial muscle.

Key words: Carbon nanotube fiber, sheath-run structure, electromechanical response, pre-twisted artificial muscle

Peer-review under responsibility of the organizing committee of SMART 2023.
doi: 10.7712/150123.9946.444746

1 INTRODUCTION

Organisms in nature can rely on muscle tissue in their bodies to move quickly and flexibly. Inspired by biological muscles, people are committed to developing new driving materials to apply to soft robots[1], artificial exoskeletons[2], prosthetics[3] and other fields to replace traditional hydraulic and electrical devices. In recent years, fibrous actuators, such as CNTs[4], graphene fibers[5], and polymer fibers[6], have attracted much attention due to their large stroke and high energy density[7, 8].

CNT fibers[9] are macroscopic fibers assembled from millions of one-dimensional continuous CNTs. The unique assembly structure brings complex interface characteristics, which endow CNT fibers with excellent actuation performance and diverse actuation methods. In 2011, Ray H. Baughman[10] found that twisted carbon nanotube fibers can generate rotations up to 590r/min in an electrolyte solution, and first proposed to use them as micromotors and artificial muscles. Subsequently, other scholars have developed twisted CNT fibers with various driving methods such as electromagnetic[11], electrothermal[12] and solvent[13]. Among them, electrothermal-electromagnetic driven CNT fibers can be used in the air and the stimulation method is simple, so they have great potential application value, but their small driving deformation (<1%) is far from meeting the actual use requirements. In order to solve this problem, Cao[14] twisted it for a second time and obtained a coiled structure similar to a spring, which amplifies the shrinkage deformation of the CNT fiber into the reduction of the pitch. For example, the paraffin-infiltrated coiled CNT fiber[15] can generate a deformation of 5.6%, this structure has also become a commonly used reinforcement method for fibrous actuators[16]. The coiled structure can amplify the deformation of the fiber on the geometric scale, but the insert of too much twist will lead to the reduction of the fiber strength[17]. More importantly, the shrinkage deformation of CNT fibers cannot be directly reflected, but is converted into the change of the pitch. Therefore, when completing a large stroke (> 10%), it is inevitable to take longer (> 10 s)[18], which is difficult to meet the response speed requirements of future drivers.

The twist of CNT fibers gradually decreases from the surface to the core, so the CNTs in the core cannot effectively participate in actuation. To solve this problem, Ray H. Baughman[19] proposed a sheath-like driving structure to effectively utilize the volume expansion effect of the guest sheath. The unit mass average mechanical energy output of sheath-run artificial muscle(SRAM) fibers is 2.9 times the mass of the same fiber/object mass than that of the filled composite muscle fiber. For twisted SRAMs, the improved actuation performance is due to the thermal softening and the thermal expansion of the guest sheath. However, under the stimulation of weak electric current, the phenomenon of improving CNT fiber actuation performance by the guest sheath cannot be explained by reported mechanisms, because the Joule heat generated by the core CNT fiber cannot heat the guest sheath to produce enough expansion and softening to release the internally torsional energy. Therefore, there should be a more complex interaction mechanism between the guest sheath and the core CNT fiber.

Herein, we report a novel densification mechanism for the guest sheath how to improve the actuation performance of CNT fiber. This improving phenomenon may be due to the shrinkage stress distributed in the radial direction of the CNT fiber when the sheath is cured, which reduces the distance between inner CNTs, thereby increasing the collective Ampere tensile force. The temperature of the guest sheath was slightly increased by exogenous heating, and the contraction actuation of the SRAMs cannot be observed; However, heating by Joule Heat at the same temperature, it can be observed that the actuation performance of SRAMs has been improved compared to the pure CNT artificial muscle fiber, which indicates that, under weak electric current, the guest sheath has a unique improving mechanism for the core CNT fiber that is different from thermal expansion and thermal softening. The changes in electrical and mechanical properties of CNT fiber before and after sheathing also support the existence of this densification transition. This mechanism can further complement the working mechanism of SRAMs and provide new ideas for its improvement.

2 RESULTS AND DISCUSSION

2.1 Fabrication and actuation mechanism of the CNT fibers@PDMS

Figure 1a is a schematic diagram of the preparation process of CNT fibers@PDMS (See Experimental Section for details). The thickness of the sheath can be adjusted by the number of coating times.

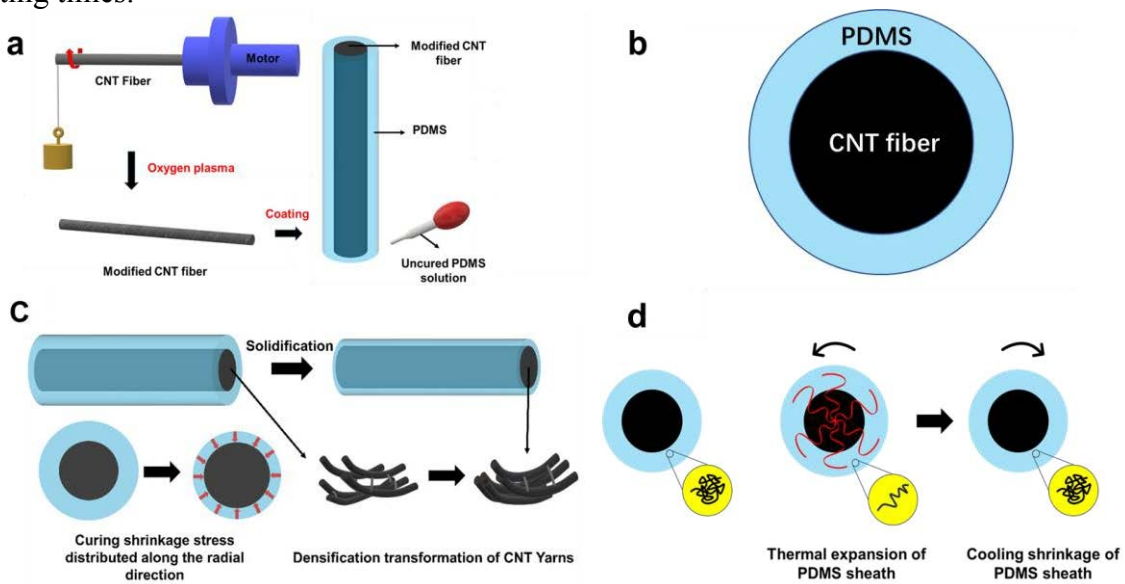

Figure 1. Schematic diagram of the fabrication process and driving mechanism of CNT fiber@PDMS. (a) Flow chart of the fabrication of CNT fiber@PDMS. (b) Schematic diagram of the cross-section of the CNT fiber@PDMS. (c) Mechanism of densification of PDMS sheath on CNT fiber (d) Untwisting shrinkage deformation mechanism of thermal expansion of PDMS sheath.

Figure 1b is a schematic cross-sectional view of CNT fibers@PDMS. The densification effect of PDMS sheath on CNT fibers and its own thermal expansion effect are of great significance to the shrinkage actuation process of CNT fibers. As shown in Figure 1c, when the driving current is small, the electrothermal effect of CNT fiber is weak and can not significantly cause the expansion of PDMS sheath. Instead, the compressive stress generated by the curing of PDMS sheath on the surface of CNT fiber reduces the distance between CNTs in CNT fiber and increases the ampere force to improve the shrinkage performance; as shown in Figure 1d, when the actuation current increases, the electrothermal effect of CNT fiber is obvious, and the PDMS sheath expands and untwists when heated. Therefore, the rotation shrinkage deformation of PDMS sheath coordinated with the core CNT fiber is generated, which avoids the use of coiled structure to improve the shrinkage deformation performance of CNT fiber.

2.2 Characterization of CNT fiber@PDMS

Figure 2a is the image of the CNT fiber after twisting. When the twist angle is 27°, the contraction output force of the CNT fiber was the maximum, and the diameter of the CNTfiber was 40 μm.

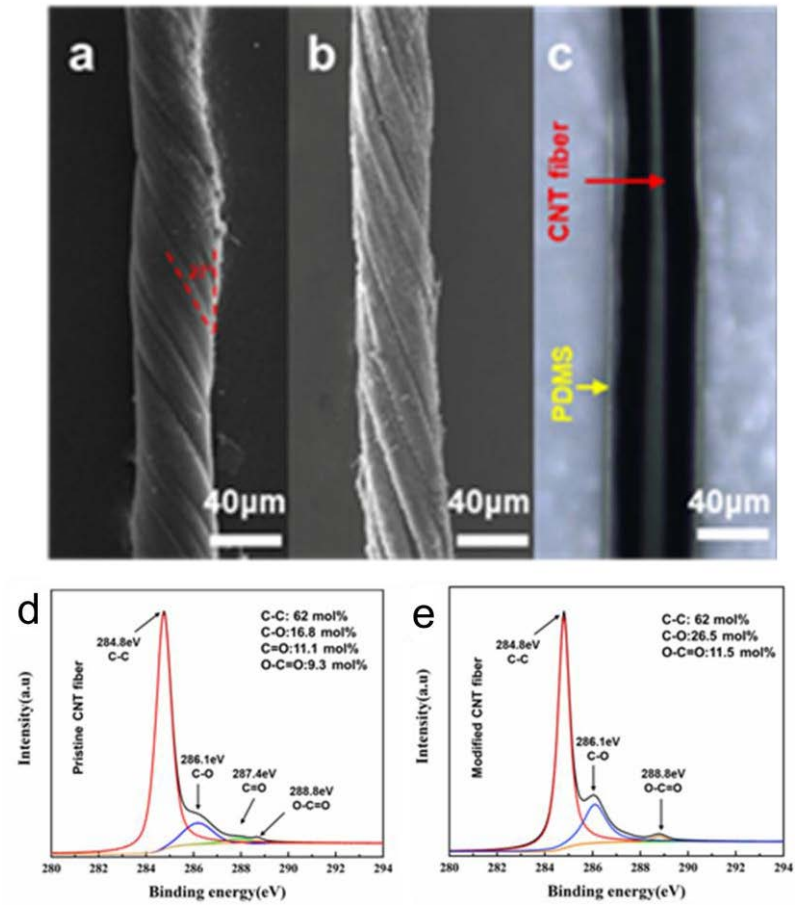

Figure 2. Photographs of fibers and changes in surface functional groups after oxygen plasma modification. (a) SEM image of the twisted CNT fiber. (b) SEM image of CNT fiber after oxygen plasma treatment. (c) Optical microscope image of CNT fiber@PDMS uncoated carbon paste. (d) C1s peak of the original CNT fiber.. (e) C1s peak of CNT fiber after oxygen plasma treatment.

Figure 2c is the optical microscope photos of CNT fibers@PDMS. The thickness of PDMS sheath was measured to be 6.7 μm, and it was successfully coated on the surface of CNT fiber.The surface of CNT fiber is chemically inert and often has the problem of poor interface bonding with other materials[20]. To improve the bonding between CNT fibers and PDMS, CNT fiber was modified by oxygen plasma. As shown in Figure 2b, the surface roughness of the modified carbon nanotube fiber increases, which was caused by the oxygen plasma bombarding the fiber surface. After measurement, the contact angle between CNT fiber and PDMS was reduced from 30 ° to 21.8 °， and the actuation and mechanical properties of CNT fibers before and after modification were not significantly affected The XPS results in Figure 2d and Figure 2e show that after oxygen plasma treatment, the oxygen content on the surface of CNT fiber increases by 1.19 mol%. Calculating the area of each Gauss peak, it is found that C = O is transformed into C-O (increased by 9.7 mol%) and O-C=O (increased by 2.2

mol%), and the content of polar functional groups on the fiber surface increases, making the interface between the two better.

2.3 Deformation properties of CNT fiber@PDMS

Figure 3a and Figure3b are the comparison diagrams of the contraction actuation stress and contraction actuation strain of CNT fibers and CNT fibers@PDMS under the current shown in Figure 3c, respectively. As shown in Figure 3d, the CNT fiber@PDMS also exhibited excellent cycling stability, with no decrease in the actuation output force value when continuously used for 1200 s under a current signal of 40 mA (0.167 Hz). As shown in Figure 3e, the electronically controlled switch designed based on the rapid shrinkage characteristics of CNT fiber@PDMS can quickly realize the “on” and “off” of the circuit under the stimulation of electrical signals, which expands the multi-functionality of CNT fiber@PDMS. application.

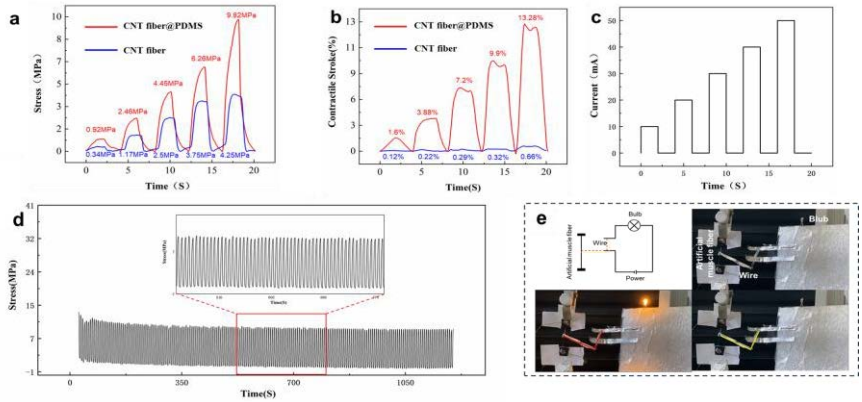

Figure 3. Bidirectional deformation characteristics of CNT fibers@PDMS and its application in circuit control. (a) Comparison of contraction stress of CNT fibers@PDMS and CNT fibers at different currents. (b) Comparison of contraction deformation of CNT fibers@PDMS and CNT fibers at different currents. (c) Current signals used for CNT fiber@PDMS and CNT fiber actuation tests. (d) Contraction cycling stability of CNT fibers@PDMS. (e) Contraction cycling stability of CNT fibers@PDMS.

2.4 Effect of temperature on fiber driving

When the CNT fiber@PDMS is charged with electric current, the CNT fiber in the core generates Ampere force[11] and also generates Joule heat[20] to expand the PDMS sheath. Therefore, the temperature has an important influence on the working mechanism of the CNT fiber@PDMS contraction. Figure 4a shows the comparison of the actuation temperature of CNT fibers@PDMS and CNT fibers at different currents (10mA-50mA). When the actuation current is 10mA and 20mA, the Joule heating effect of CNT fibers is not obvious (At 10mA and 20mA, the fiber temperature increased by 3°C and 15°C compared with room temperature, respectively). In order to explore the contraction mechanism of CNT

fiber@PDMS at low current, the CNT fiber@PDMS was stretched at a speed of 0.01 mm/min after applying a load of 3 mN. Irradiation heating to 40 ℃(10s) and cooling to 25 ℃(10s) were used to change the temperature alternately, and then the change of load was observed. As shown in Figure 4b, the surface temperature of the CNT fiber@PDMS gradually increased to 40 °C with the irradiation, but the load value decreased instead, so there was no contraction occurred, which was also observed when heating the CNT fibers in our previous study[21]. This phenomenon is solved because the modulus of the CNT fiber@PDMS decreases after thermal. At this time, the PDMS sheath does not contribute to the contraction of the CNT fiber@PDMS, but mainly the amperometric force of the core CNT fiber produces the contraction.

With the increase of driving current, the Joule heating effect of CNT fiber gradually increases, and the temperature of CNT fibers@PDMS was higher than that of CNT fibers, which may be the thermal insulation effect of PDMS sheath. At 50 mA current, the temperature of CNT fiber@PDMS increased by 108 °C compared with room temperature. To explore the contraction mechanism of CNT fiber@PDMS at higher currents, a heat gun was used to provide higher heating temperatures. As shown in Figure 4c, during the heating process of CNT fiber@PDMS from 55 °C to 158.3 °C, a significant contraction deformation (12.3%) occurred, which was mainly caused by the thermal expansion effect of PDMS sheath, and the core CNT fiber mainly provides heat for PDMS sheath.

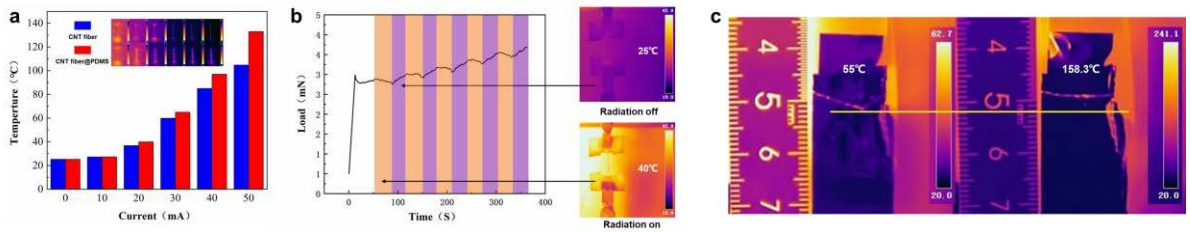

Figure 4. Temperature and heating effect of CNT fiber@PDMS on its contraction behavior at different currents. (a) Temperature of CNT fiber@PDMS at different currents. (b) Variation of loading value of CNT fiber@PDMS under radiative alternating heating (25°C-40°C). (c) Contraction deformation of CNT fiber@PDMS under heat gun heating (55°C-158°C).

2.5 Densification of CNT fiber by PDMS sheath

From the conclusion in Section 2.4, it can be seen that during the contraction process of CNT fibers@PDMS under lower current, the PDMS sheath cannot contribute to the contraction, but will produce deformation resistance to the CNT fibers in the core. Compared with the CNT fibers, the actuation stress and actuation strain were not decreased but significantly increased. This was because the PDMS sheath will generate shrinkage stress uniformly distributed along the radial direction of the CNT fibers during the curing process, which will reduce the CNTs spacing inside the CNT fiber, and the amperometric force between the CNTs can be calculated using the formula (1) and (2) to represent:

$$\rightarrow = \frac{\mu_0}{4\pi} \frac{I \quad \vec{l} \times \vec{r}}{r^3} \tag{1}$$

$$F = \quad IdL \sin \alpha \tag{2}$$

where B is the magnetic flux generated by energized CNTs, μ_0 is the magnetic permeability between CNTs, r is the distance between adjacent CNTs, F is the ampere force between the CNTs, I is the current passing through the CNTs, and α is the angle between the direction of the current flowing into the CNT and the direction of the magnetic field generated by the surrounding CNTs. The densification of the PDMS sheath reduces the distance r between CNTs and increases the ampere force F, which enhancing effect on the actuation performance of CNT fibers was much greater than its deformation resistance to CNT fibers in the process of contraction. Therefore, the actuation performance of the CNT fiber@PDMS far more than CNT fibers. To demonstrate the densification effect of the PDMS sheath on the CNT fiber, the modulus-strain curves and resistivity of the CNT fiber@PDMS were tested.

CNT fibers has a complex multi-level structure[22], and its modulus is closely related to the change of internal structure[23-25]. In the tensile process, firstly, the CNT inside CNT fibers is loose and non oriented, and the CNT is gradually aligned under the action of stress. At this time, the fiber modulus increases. This stage is also known as "a straining region" (① in Figure 5d and Figure 5e); Then, the internal CNT orientation is consistent, and the elastic modulus of CNT fiber reaches the maximum; In the subsequent tensile process, some CNTs break, and the elastic modulus of CNT fibers begins to decrease (② in Figure 5d and Figure 5e). Park[26] used the mechanical model of biomaterials to analyze the modulus-strain curve of CNT fibers, and found that the more densely structured CNT fibers correspond to the greater the extreme value of the elastic modulus. Figures 5a and Figure 5b are the stress-strain curves of CNT fibers and CNT fibers@PDMS, respectively. The modulus-strain curves of CNT fiber (Figure 5d) and CNT fiber@PDMS (Figure 5e) can be obtained by derivation. Since the PDMS sheath and the CNT fiber are co-deformed during the stretching process, the modulus of the core CNT fiber cannot be directly obtained. Through stress analysis and calculation, it can be obtained that the modulus of CNT fiber after wrapping PDMS sheath was increased from 118Mpa to 780Mpa.

According to Figure 5c, the resistivity of CNT fibers decreased by 18% (from 0.83 Ω/mm to 0.68 Ω/mm) after coating with PDMS sheath. Previous studies have proved that the conduction of electrons in CNT fibers mainly includes two ways: intra-tube conduction and inter-tube conduction, and the resistance of electron conduction in the CNTs is much smaller than that in the conduction between the CNT, so the resistance of the CNT fiber is mainly due to the factor of the transmission between the CNTs. Decide. Currently, two theoretical models, Variable range hopping (VRH)[27, 28] and Fluctuation induced tunneling (FIT)[29, 30], are considered to be the main mechanisms for electron transfer between CNTs, and in these two models, the reduction of the distance between CNTs can increase the probability of electron jumping or tunneling between CNTs.

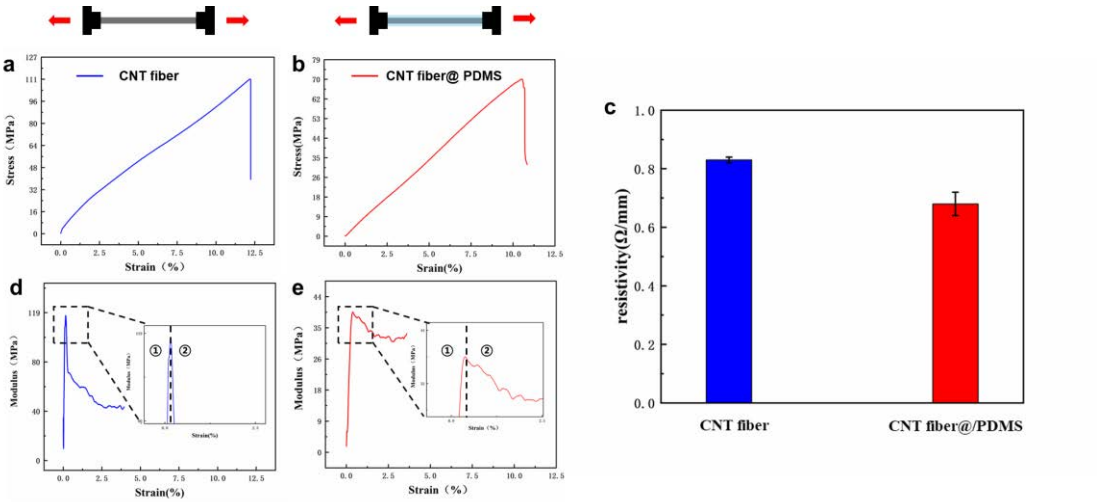

Figure 5. The effect of PDMS sheath on the mechanical and electrical properties of the core CNT fiber. (a) Stress-strain curve of the CNT fiber. (b) Stress-strain curves of CNT fiber@PDMS. (c) Variation of resistance between CNT fiber and CNT fiber@PDMS. (d) Modulus-strain curve of the CNT fiber. (e) Modulus-strain curves of CNT fiber@PDMS.

3 CONCLUSION

To summarize, a pre-twisted CNT fiber@PDMS based on a sheath-like structure can produce a tensile stroke of 13.28% at a very fast rate under electric current of 50 mA. The improved actuation performance was attributed to the enhancement effect of the PDMS sheath on the core fiber, which has different mechanisms under various electric currents. Under weak currents, the Joule heat generated by the core CNT fiber does not cause significant thermal softening and thermal swelling of the PDMS sheath to release the stored torsional energy, but rather increases the collective Ampere force through a radial shrinkage stress during curing. Conversely, with the increasing of electric current, the thermal softening and thermal swelling of the PDMS sheath releases the stored torsional energy, thus improving the overall actuation performance of the CNT fiber@PDMS.

4 EXPERIMENTAL SECTION

4.1 Materials

CNT fibers, Hebei Tanyuan nanotechnology Co.,Ltd; PDMS, Mn = 3000, gelest, USA; 2,6-pyridydicarbonyl chloride ($C_7H_3Cl_2NO_2$,96%), Shanghai Aladdin Biochemical Co., Ltd; Zinc trifluoromethanesulfonate (Zn $(OTf)_2$,98%), Shanghai Aladdin Biochemical Co., Ltd; Triethylamine (TEA, AR), Tianjin Fuyu Fine Chemical Co., Ltd; Dichloromethane (CH_2Cl_2, AR), Tianjin Fuyu Fine Chemical Co., Ltd; Anhydrous methanol (CH_3OH, AR), Tianjin

Damao Chemical Reagent Factory; Anhydrous ethanol (C_2H_5OH, AR), Xilong Chemical Co., Ltd.

4.2 Fabrication of sheath-like CNT fiber@PDMS

Preparation of uncured PDMS solution

Using nitrogen as protective gas, 15 g of PDMS capped by aminopropyl group was dissolved in 20 ml dichloromethane, 3 ml triethylamine was added at 0 ℃ and stirred for 2 h. 1.02 g of 2,6-pyridinedicarbonyl chloride was dissolved in 10 ml dichloromethane and added to the above solution for 2 h. After stirring at room temperature for 2 days, 40 ml methanol was added to terminate the reaction. The product was placed in a vacuum drying oven to remove the solvent.

Oxygen plasma treatment of CNT fiber

5cm CNT fiber was placed horizontally, one end was connected with a weight to prevent crimping, and the other end was connected with a stepping motor to twist the fiber to shorten the length by 20%.

Then the CNT fiber was modified by oxygen plasma. The modified equipment (k1050x) was provided by Quorum company in the UK. The gas flow rates of oxygen and helium are 0.3L/min and 30L/min respectively and processing time of CNT fibers is 4 s.

Preparation of PDMS sheath on CNT fiber

The sheath was deposited at room temperature on CNT fiber by manually drawing droplets of the uncured PDMS solution along the length of the vertically. 1cm uncoated part should be reserved at both ends of CNT fiber to connect copper wire. After waiting for PDMS curing at room temperature, the flexible carbon paste should be evenly coated on the surface of PDMS layer to obtain Sheath-like CNT fiber@PDMS structure.

4.3Characterization and measurement

Laser confocal microscope (OLS4100, Olympus) was used to characterize the morphology of the CNT fiber@PDMS. The morphology of CNT fiber and modified CNT fiber was characterized by SEM (Supra 55, Zeiss). The changes of surface functional groups of CNT fiber after oxygen plasma modification were measured by XPS (ESCALAB Xi+, Thermo). The stress-strain curve and modulus-strain curve of CNT fiber and CNT fiber@PDMS were measured by universal tensile testing machine (HY-0580, Hengyi). The temperature of CNT fiber@PDMS was calibrated by infrared thermal imager (615C, Fotric) and supporting software. The resistivity of fiber before and after coating PDMS sheath was measured by high-precision digital multimeter (Dmm6500, Keithley).

In order to characterize the deformation during contraction, the CNT fiber@PDMS and CNT fibers were placed horizontally, and the laser displacement sensor (HG-C1030, Panasonic) was fixed below. The laser spot was caught by hanging a square piece of paper in

the middle of the fiber. The programmable direct-current (DC) power supply (36-03, Hspy) was used to provide DC current for the core CNT fiber.

The actuation stress and the change of CNT fibers load by heat are measured by universal tensile testing machine with 1N stress sensor (Futek LSB 200), in which 0.003N load was provided to keep the CNT fiber in a straight state, and then the change of force value is measured at the tensile rate of 0.01mm/min to prevent the influence of creep on the results.

ACKNOWLEDGMENTS

The authors acknowledge the financial support obtained from the National Key Research and Development Program of China (2020YFB1312900) and the National Natural Science Foundation of China (21975281).

AUTHOR CONTRIBUTIONS

Zenghui Zhao: Methodology, Preparation, Test, Writing – original draft. Sufeng Zhu: Mechanism. Xufeng Dong: Supervision, Conceptualization, Writing – review & editing. Min Qi: Validation. Hao Huang: Oxygen plasma modification. All authors contributed to the article and approved the submitted version.

DECLARATION OF INTERESTS

The authors declare no competing interests.

REFERENCES

[1] C. Laschi, B. Mazzolai, and M. Cianchetti, "Soft robotics: Technologies and systems pushing the boundaries of robot abilities," (in English), *Sci Robot,* vol. 1, no. 1, Dec 6 2016. [Online]. Available: <Go to ISI>://WOS:000441507900003.

[2] G. Z. Yang *et al.*, "The grand challenges of Science Robotics," (in English), *Sci Robot,* vol. 3, no. 14, Jan 24 2018. [Online]. Available: <Go to ISI>://WOS:000441684500006.

[3] D. Rus and M. T. Tolley, "Design, fabrication and control of origami robots," *Nature Reviews Materials,* vol. 3, no. 6, pp. 101-112, 2018, doi: 10.1038/s41578-018-0009-8.

[4] Q. Li, X. Wang, L. Dong, C. Liu, and S. Fan, "Spirally deformable soft actuators and their designable helical actuations based on a highly oriented carbon nanotube film," *Soft Matter,* vol. 15, no. 47, pp. 9788-9796, Dec 4 2019, doi: 10.1039/c9sm01966a.

[5] J. Foroughi and G. Spinks, "Carbon nanotube and graphene fiber artificial muscles," *Nanoscale Advances,* vol. 1, no. 12, pp. 4592-4614, 2019, doi: 10.1039/c9na00038k.

[6] Y. Dou *et al.*, "Artificial spider silk from ion-doped and twisted core-sheath hydrogel fibres," *Nat Commun,* vol. 10, no. 1, p. 5293, Nov 22 2019, doi: 10.1038/s41467-019-13257-4.

[7] J. Xiong, J. Chen, and P. S. Lee, "Functional Fibers and Fabrics for Soft Robotics, Wearables, and Human-Robot Interface," *Adv Mater,* vol. 33, no. 19, p. e2002640, May 2021, doi: 10.1002/adma.202002640.

[8] M. Zou *et al.*, "Progresses in Tensile, Torsional, and Multifunctional Soft Actuators," *Advanced Functional Materials,* vol. 31, no. 39, 2021, doi: 10.1002/adfm.202007437.

[9] Y. Wu, X. Zhao, Y. Shang, S. Chang, L. Dai, and A. Cao, "Application-Driven Carbon Nanotube Functional Materials," *ACS Nano,* vol. 15, no. 5, pp. 7946-7974, May 25 2021, doi: 10.1021/acsnano.0c10662.

[10] J. Foroughi *et al.*, "Torsional Carbon Nanotube Artificial Muscles," (in English), *Science,* vol. 334, no. 6055, pp. 494-497, Oct 28 2011. [Online]. Available: <Go to ISI>://WOS:000296230500042.

[11] W. Guo *et al.*, "A novel electromechanical actuation mechanism of a carbon nanotube fiber," *Adv Mater,* vol. 24, no. 39, pp. 5379-84, Oct 9 2012, doi: 10.1002/adma.201201845.

[12] M. D. Lima *et al.*, "Electrically, Chemically, and Photonically Powered Torsional and Tensile Actuation of Hybrid Carbon Nanotube Yarn Muscles," (in English), *Science,* vol. 338, no. 6109, pp. 928-932, Nov 16 2012. [Online]. Available: <Go to ISI>://WOS:000311083600038.

[13] K. Jin *et al.*, "Self-plied and twist-stable carbon nanotube yarn artificial muscles driven by organic solvent adsorption," *Nanoscale,* vol. 10, no. 17, pp. 8180-8186, May 3 2018, doi: 10.1039/c8nr01300d.

[14] Y. Shang *et al.*, "Super-stretchable spring-like carbon nanotube ropes," *Adv Mater,* vol. 24, no. 21, pp. 2896-900, Jun 5 2012, doi: 10.1002/adma.201200576.

[15] Y. Shang *et al.*, "Large-Deformation, Multifunctional Artificial Muscles Based on Single-Walled Carbon Nanotube Yarns," *Advanced Engineering Materials,* vol. 17, no. 1, pp. 14-20, 2015, doi: 10.1002/adem.201400163.

[16] C. Lamuta, S. Messelot, and S. Tawfick, "Theory of the tensile actuation of fiber reinforced coiled muscles," *Smart Materials and Structures,* vol. 27, no. 5, 2018, doi: 10.1088/1361-665X/aab52b.

[17] J. C. Anike, K. Belay, and J. L. Abot, "Effect of twist on the electromechanical properties of carbon nanotube yarns," *Carbon,* vol. 142, pp. 491-503, 2019, doi: 10.1016/j.carbon.2018.10.067.

[18] L. Xu *et al.*, "Artificial muscle with reversible and controllable deformation based on stiffness-variable carbon nanotube spring-like nanocomposite yarn," *Nanoscale,* vol. 11, no. 17, pp. 8124-8132, Apr 25 2019, doi: 10.1039/c9nr00611g.

[19] J. K. Mu *et al.*, "Sheath-run artificial muscles," (in English), *Science,* vol. 365, no. 6449, pp. 150-+, Jul 12 2019. [Online]. Available: <Go to ISI>://WOS:000474905400039.

[20] F. Meng *et al.*, "Electro-induced mechanical and thermal responses of carbon nanotube fibers," *Adv Mater,* vol. 26, no. 16, pp. 2480-5, Apr 23 2014, doi: 10.1002/adma.201305123.

[21] S. Zhu, J. Di, Z. Zhao, X. Dong, and M. Qi, "A structure evolution mechanism for the modulus loss in electromechanical response of carbon nanotube fiber," *Carbon,* vol. 185, pp. 289-299, 2021, doi: 10.1016/j.carbon.2021.09.023.

[22] J. Park and K.-H. Lee, "Carbon nanotube yarns," *Korean Journal of Chemical Engineering,* vol. 29, no. 3, pp. 277-287, 2012, doi: 10.1007/s11814-012-0016-1.

[23] Q. Li *et al.*, "Multi-scale study of the strength and toughness of carbon nanotube fiber materials," *Materials Science and Engineering: A,* vol. 549, pp. 118-122, 2012, doi: 10.1016/j.msea.2012.04.015.

[24] T. H. Nam, K. Goto, Y. Shimamura, Y. Inoue, and S. Ogihara, "Property improvement of CNT spun yarns and their composites through pressing, stretching and tensioning," *Advanced Composite Materials,* vol. 28, no. 5, pp. 507-524, 2019, doi: 10.1080/09243046.2019.1610586.

[25] G. Sun, D. Wang, J. H. L. Pang, J. Liu, and L. Zheng, "Nonlinear stress-strain behavior of carbon nanotube fibers subject to slow sustained strain rate," *Applied Physics Letters,* vol. 103, no. 13, 2013, doi: 10.1063/1.4822112.

[26] J. Park *et al.*, "Mathematical model for the dynamic mechanical behavior of carbon nanotube yarn in analogy with hierarchically structured bio-materials," *Carbon,* vol. 152, pp. 151-158, 2019, doi: 10.1016/j.carbon.2019.05.077.

[27] S. Luo, T. Liu, S. M. Benjamin, and J. S. Brooks, "Variable range hopping in single-wall carbon nanotube thin films: a processing-structure-property relationship study," *Langmuir,* vol. 29, no. 27, pp. 8694-702, Jul 9 2013, doi: 10.1021/la401264r.

[28] D. P. Wang *et al.*, "Hopping conduction in disordered carbon nanotubes," *Solid State Communications,* vol. 142, no. 5, pp. 287-291, 2007, doi: 10.1016/j.ssc.2007.02.028.

[29] O. S. Dewey *et al.*, "Transport and photo-conduction in carbon nanotube fibers," *Applied Physics Letters,* vol. 115, no. 2, 2019, doi: 10.1063/1.5089003.

[30] J. Gao and Y.-L. L. Loo, "Temperature-Dependent Electrical Transport in Polymer-Sorted Semiconducting Carbon Nanotube Networks," *Advanced Functional Materials,* vol. 25, no. 1, pp. 105-110, 2015, doi: 10.1002/adfm.201402407.